

doi:10.15199/48.2018.01.07

# Numerical Solution of Electroheat Problems with Time-varying Geometries

**Abstract.** Novel approach to modeling of 3D coupled electroheat problems with time-varying geometries is presented. Instead of time-expensive remeshing of the whole system in every time step it is used the initial mesh that takes into account the expected geometric changes. In the course of computations, its relevant elements are able to adaptively change their shapes and material parameters. The methodology is illustrated with an example of induction-assisted laser cladding.

**Streszczenie.** W artykule przedstawiono nowe podejście do trójwymiarowego modelowania problemów elektrotermicznych ze zmiennymi w czasie geometriami. Zamiast stosowania czasochłonnnych metod remeshingu w każdym kroku czasowym wprowadzono początkową siatkę, biorącą pod uwagę oczekiwane zmiany geometryczne. W procesie obliczania istotne elementy siatki są w stanie adaptacyjnie zmieniać ich kształt i parametry materiałowe. Przedstawiona metodologia została zilustrowana przykładem wspomaganego indukcyjnie okładzinowania laserowego. (**Rozwiązanie numeryczne problemów elektrotermicznych ze zmienną w czasie geometrią**)

**Keywords:** coupled problems, electroheat, time-varying geometry, numerical analysis, cladding

**Słowa kluczowe:** problem sprzężone, elektrotermia, zmienna w czasie geometria, analiza numeryczna, okładzinowanie

## Introduction

Some modern electroheat technologies work with continuous delivery of material (coming, for instance, from welding rods or metal powder) in the course of the process and this material in different forms (liquid or solid) must also be considered in the corresponding models. As some parts of the system during the operation move, the classical way of computation was based on full remeshing of the solved model in every time step and assigning new material properties to cells containing it (moreover, the shape of particular elements with added material is not known in advance) and had to be estimated. In 3D, however, this procedure is generally very expensive. The paper presents an alternative algorithm of solving the problem locally, which is based on a simple adaptive technique.

Let us illustrate the problem on laser cladding [1–4]. This process belongs to the best techniques of depositing material on a substrate with the aim to improve the surface properties (hardness, corrosion and/or wear resistance) or renovation of the damaged areas. Laser beam heats metal powder added by a nozzle and the powder melts together with the surface layer of the substrate, thus producing a melt pool. After its solidification, a track is created, containing mixture of the substrate and added powder metals. A series of parallel tracks then forms the deposited layer. The technology is mostly applied on either planar or cylindrical surfaces.

The process of laser heating is characterized by extremely high temperature gradients. As the temperature of the surface irradiated by laser beam reaches 2000 °C in about 1–2 s, its gradient exceeds even more than 1000 °C/s. This may lead, however, after cooling to subsequent mechanical stresses of thermoelastic or thermoplastic origin in the processed material. But their presence is highly undesirable, as they may cause, for instance, cracks or peeling off the cladded tracks.

One of suitable methods for suppressing so high values of the above gradient is induction preheating of the substrate (but its induction postheating is also possible). This technique can reduce the temperature gradients to one half of their original value and even more, which substantially reduces the above stresses

A typical arrangement of cladding is indicated in the left part of Fig. 1. Here, the substrate (for example a steel plate) is supposed to move at a low velocity  $v$  in the indicated

direction, while the laser head with the nozzle delivering the powder material are unmovable. The substrate is preheated by the inductor (that should be as near the laser beam as possible in order to avoid the undesirable decrease of temperature). The laser beam melts both the surface layers of the substrate and the powder. Hence, a pool is produced containing a mixture of both components. As the substrate moves, the pool gets farther from the place irradiated by the laser beam and starts solidifying, also very fast (heat is transferred to the interior of the substrate). The cross section of the track is depicted in the right part of Fig. 1.

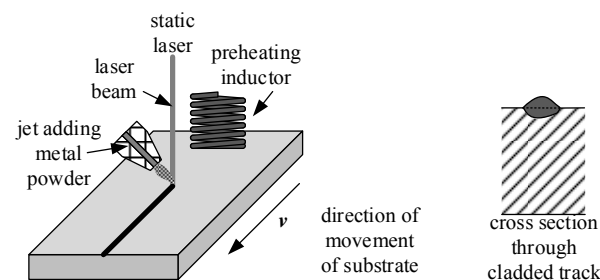


Fig. 1. Laser cladding with induction preheating

Unfortunately, the shape of this cross section is not known in advance and depends on a lot of parameters (power of laser beam, velocity of motion of the substrate, temperature of preheating, injection rate of delivered powder etc.). It can be seen that the technique of mere remeshing the system with estimation of the shape of track may lead to unacceptable errors.

## Formulation of the technical problem

First, let us explain why it is necessary to model the process before realizing it in practice. It is clear that the deposited layer on either planar or cylindrical surface must be as uniform and smooth as possible in order to avoid subsequent expensive machining (the deposited layer is, moreover, very hard). Practically, after finishing the process of cladding, we can obtain three kinds of results depicted in Fig. 2.

Again, the cross section through several parallel tracks can look like one of the depicted cases, which depends not only on the above parameters, but also on the set distance between the longitudinal axes of individual tracks. The left part of Fig. 2 shows the case characterized by higher ve-

locity  $\nu$  leading to production of separate tracks (unacceptable result), middle part shows the acceptable shape of the deposited layer, while the right part depicts higher (and also unacceptable) interferences of the tracks caused by either very low velocity  $\nu$  of the substrate or excessive powder injection rate.

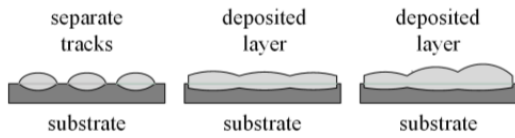


Fig. 2. Possible results of process of cladding (transverse cross section)

It can be seen, that the task is extremely complicated, as it should also include the backward problem for determining the optimized parameters leading to a uniform and smooth deposited layer.

The goal of this paper is to present the algorithm for solving the forward task using a better and time saving algorithm for finding the resultant shape of particular tracks, and illustrate it with a typical example.

### Mathematical model

The forward task represents a strongly nonlinear and non-stationary 3D electro-thermal problem, characterized by continuous addition of powder material and geometrical changes that are unknown in advance. It is necessary to model magnetic field generated by the preheating inductor and temperature fields produced by both the inductor and laser beam.

- *Magnetic field generated by the inductor*

The magnetic field in the system is described by the equation for the magnetic vector potential  $\mathbf{A}$  [5, 6]

$$(1) \quad \text{curl} \left( \frac{1}{\mu} \text{curl} \mathbf{A} \right) + \gamma \left( \frac{\partial \mathbf{A}}{\partial t} - \nu \times \text{curl} \mathbf{A} \right) = \mathbf{J}_{\text{ext}},$$

where  $\mu$  is the magnetic permeability,  $\gamma$  denotes the electric conductivity and  $\mathbf{J}_{\text{ext}}$  stands for the vector of the external harmonic current density in the field coil. But solution to (1) is, in this particular case, practically unfeasible. The reason consists in a deep disproportion between the frequency  $f$  (usually hundreds of Hz) of the field current  $I_{\text{ext}}$  and time of heating  $t_{\text{H}}$  (usually several seconds). That is why the model was somewhat simplified using two assumptions. The first of them is based on the fact, that the velocity  $\nu$  of motion is low (several mm/s). The second one considers the magnetic field harmonic. In such a case, it can be described by the Helmholtz equation for the phasor  $\underline{\mathbf{A}}$  of the magnetic vector potential  $\mathbf{A}$  in the form

$$(2) \quad \text{curl}(\text{curl} \underline{\mathbf{A}}) + j \cdot \omega \gamma \mu \underline{\mathbf{A}} = \mu \underline{\mathbf{J}}_{\text{ext}}$$

and solved in the frequency domain.

Here,  $\omega$  denotes the angular frequency ( $\omega = 2\pi f$ ). But the magnetic permeability  $\mu$  of ferromagnetic parts is supposed not to be a constant everywhere; in every cell of the discretization mesh containing ferromagnetics it is assigned to the local average value of the magnetic flux density. Its computation is, in such a case, based on an appropriate iterative procedure.

The conditions along the artificial boundary placed at a sufficient distance from the system are of the Dirichlet type ( $\underline{\mathbf{A}} = \mathbf{0}$ ).

- *Temperature field produced by the inductor*

The temperature field in the system is described by the heat transfer equation [7]

$$(3) \quad \text{div}(\lambda \cdot \text{grad} T) = \rho c_p \cdot \left( \frac{\partial T}{\partial t} + \nu \cdot \text{grad} T \right) - w,$$

where  $T$  is the temperature,  $\lambda$  is the thermal conductivity,  $\rho$  denotes the mass density and  $c_p$  stands for the specific heat (all of these parameters are generally temperature-dependent quantities). Finally, symbol  $w$  denotes the time average internal volumetric sources of heat that generally consist of the volumetric Joule losses  $w_j$  (due to eddy currents) and magnetization losses  $w_m$ . Thus, we can write

$$(4) \quad w = w_j + w_m,$$

where

$$(5) \quad w_j = \frac{|\underline{\mathbf{J}}_{\text{eddy}}|^2}{\gamma}, \quad \underline{\mathbf{J}}_{\text{eddy}} = -j \cdot \omega \gamma \underline{\mathbf{A}},$$

while  $w_m$  are determined from the known measured loss dependence  $w_m = w_m(|\underline{\mathbf{B}}|)$  for the material used (magnetic flux density  $\mathbf{B}$  in every element of the mesh is in this model also harmonic), or from the Steinmetz formula. In many cases, however, the magnetization losses are neglected as their value is very small (less than 10 %) with respect to the Joule losses. The boundary conditions take into account convection and radiation and may be written in the form

$$(6) \quad -\lambda \frac{\partial T_s}{\partial n} = \alpha(T_s - T_{\text{ext}}) + \sigma C(T_s^4 - T_r^4).$$

In the above equation,  $\alpha$  denotes the coefficient of convective heat transfer,  $T_s$  stands for the surface temperature,  $T_{\text{ext}}$  is the temperature of sufficiently distant ambient medium and  $n$  represents the direction of the outward normal to the surface  $S$  of the body at a given point. Symbol  $\sigma$  expresses the Stefan–Boltzmann constant,  $C$  is the coefficient of emissivity that may also include the configuration factor and influence of the multiple reflections and, finally,  $T_r$  stands for the temperature of surface to which heat from the system is radiated.

- *Temperature field produced by the laser beam*

Heating by the laser beam is considered in the form of delivery of a specified heat power to a given spot of the surface. The basic equation corresponds to (3), but now the internal volumetric losses  $w$  vanish, as heat is delivered to the material from the surface. This may be taken into account by a boundary condition that is similar to (6), but contains one more term  $q_{\text{in}}$  corresponding to the delivered thermal flux

$$(7) \quad -\lambda \frac{\partial T_s}{\partial n} = -q_{\text{in}} + \alpha(T_s - T_0) + \sigma C(T_s^4 - T_r^4)$$

Prescription of the boundary condition requires knowledge of the actual surface temperature of the body after pre-heating, which is somewhat reduced by cooling caused by the local time delay between the inductive pre-heating and laser heating.

Determining of the distribution of quantity  $q_{\text{in}}$  is, however, uneasy due to the fact that the power of the laser beam is known only at its source (its value is  $P_0$ ). The power  $P_1$  delivered to the surface of the substrate is somewhat lower ( $P_1 = kP_0$ ,  $0 < k < 1$ ). The reason is partial reflec-

tion of the beam from the substrate and also absorption in the air and mainly in a cloud of plasma produced by evaporation of molten metal from the heated spot. The coefficient  $k$  has to be found experimentally. Moreover, the intensity of laser beam decreases with the distance of its axis. That is why the distribution of  $q_{in}$  is supposed to obey the Gauss distribution, where

$$(8) \quad P_1 = \int_S q_{in} dS$$

and  $S$  is the surface of the irradiated spot.

Other fine phenomena accompanying laser heating [8] are not analyzed in this paper.

- **Deformation of the surface**

In the past, various authors proposed algorithms working with changing geometry [9–10]. But these did not seem to be suitable for the solved problem. Therefore, we proposed and tested two different algorithms that are driven by the local temperature and its gradient. In this paper, we will describe the algorithm based on DG (deformation of geometry) that is partially implemented in the professional code COMSOL Multiphysics 5.2.

The algorithm works with the definition of velocity of deformation as a function of selected parameters, in our case temperature and geometry. First we will illustrate the situation in the cross section of the substrate before, during and after the irradiation. The mesh in the cross section before irradiation is indicated in Fig. 3.

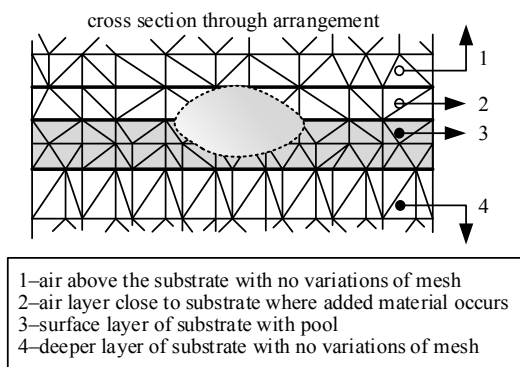


Fig. 3. Mesh in the cross section of substrate before irradiation

At the moment when the above 2D cross section is irradiated by the laser beam, the substrate layer 3 starts to be heated at a very high gradient together with added powder in zone 2. In a short time (from tenths of seconds up to few seconds) a pool of molten mixture is produced, that fast changes its dimensions (the pool is indicated by the dotted line). Now, in the place with the liquid phase the mesh must be refined and temperature in it must be recalculated. The cells in layer 2, whose temperature exceeds the point of melting of added material are supposed to be filled with this material. When the laser beam leaves this spot, the pool starts solidifying. After solidification, we obtain the arrangement in Fig. 4. The mesh is then again coarsened in order to avoid permanent growing the number of degrees of freedom.

As can be seen, the algorithm must include refinement and coarsening of the local mesh. This is assured by an implemented specific automatic  $h$ -adaptive algorithm.

Another issue is the selection of the time step. As the change of the pool in time is relatively fast, and it is impossible to solve the task with a very fine time step, it is much more convenient to consider the velocity of deformation that allows working with the mentioned DG module in COMSOL Multiphysics. In cells of discretization mesh whose tempera-

ture is lower than the melting point of materials, the velocity is equal to zero. In case that the temperature exceeds the melting point, it becomes nonzero and its velocity depends on the direction of propagation and used coordinate system (Cartesian or cylindrical) and mostly is driven by the sine or cosine law. Its amplitude, however, must be found from the experimental calibration for the given type of problem.

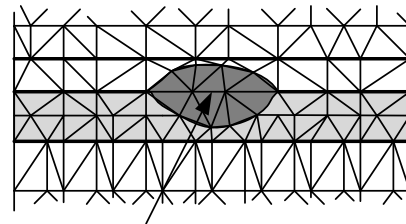


Fig. 4. Mesh in the cross section after irradiation

### Numerical solution

The numerical solution was performed using professional code COMSOL Multiphysics 5.2 supplemented with a series of own scripts and procedures. But the computations are still rather expensive (one variant takes 2.5–8 hours on a top-parameter PC, according to the degree of coupling).

### Illustrative example

Cladding of four parallel tracks (using stainless steel alloy powder Metco 41C) on an inductively preheated substrate made of steel S355 was modeled and also investigated experimentally. The cross-section of the arrangement is depicted in Fig. 5.

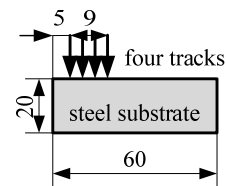


Fig. 5. Cross section through the arrangement (dimensions in mm)

- **Input data**

The substrate is represented by a steel plate of dimensions 1000×60×20 mm. The saturation curve of steel S355 at room temperature is depicted in Fig. 6. Its dependence on the temperature is taken into account and similar dependences of other material parameters are respected as well.

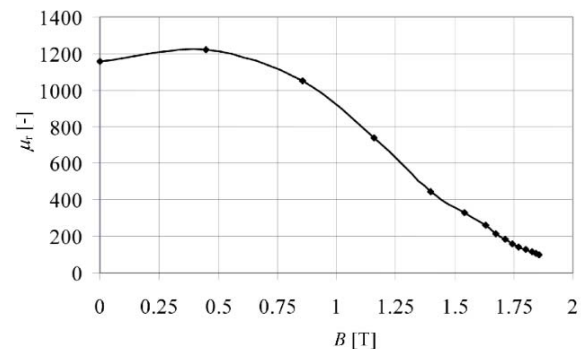


Fig. 6. Saturation curve of steel S355 (at room temperature)

The inductor is wound by one hollow massive copper turn cooled by water, placed in a composite shell made of Fluxtrol. It carries current of the amplitude 2260 A and frequency 12 kHz. The recalculated power  $P_1$  of the laser beam of diameter 3 mm (on the surface of substrate) is about 250 W, and obeys the Gauss distribution. The distan-

ce between the laser and inductor  $b = 40$  mm. The velocity of the motion is 4 mm/s and the height of the inductor above the substrate is 2 mm.

More input data, with respect to the extent of the paper, cannot be presented.

### • Results

Figure 7 shows the cross section of a single track together with the local mesh after adaptive refinement. The dimensions of cells with the pool are less than 2 mm.

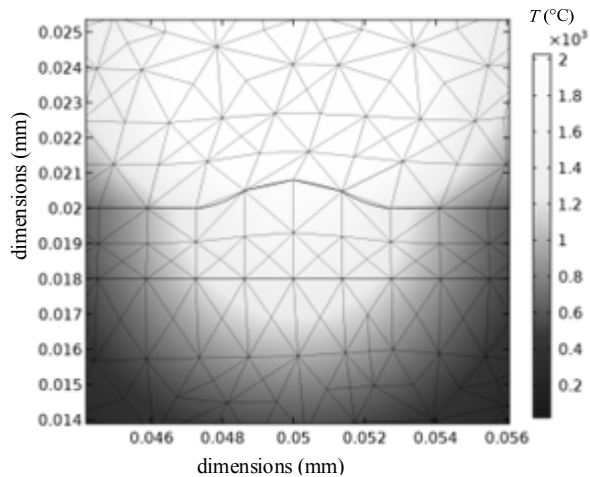


Fig. 7. Cross section through the track together with refined mesh

Figure 8 depicts the 3D view of the single track after 5 s of the cladding process.

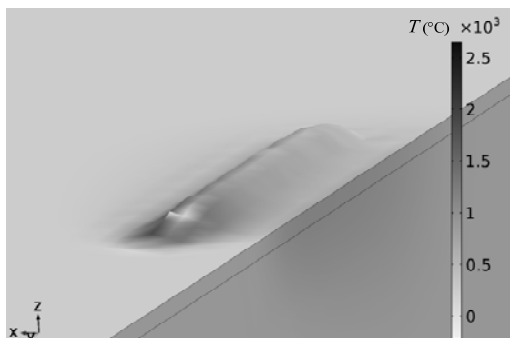


Fig. 8. First track after five seconds of cladding process

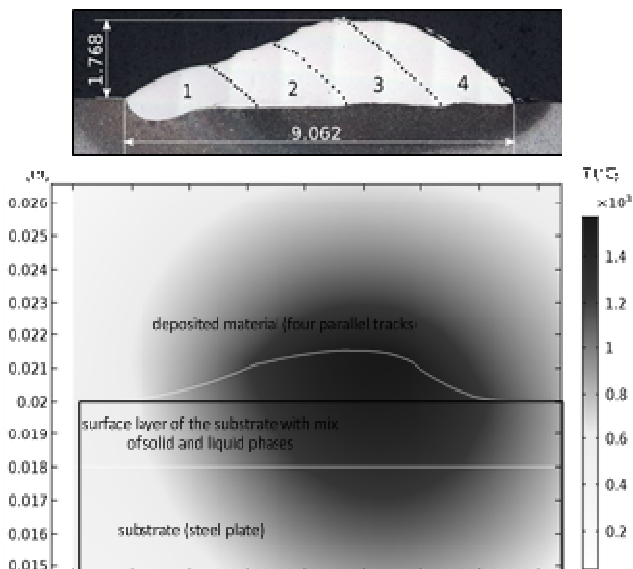


Fig. 9. Four tracks close to one another: up—measured, bottom—modeled

Finally, Fig. 9 shows the cross section through four tracks obtained by measurements (upper part) and experiment (bottom part).

### Conclusion

The paper presents an alternative method for computation of electroheat problems characterized by successive adding some material (melting rod, powder metal) to the substrate. Further work in the domain will be aimed at acceleration of the algorithm, its application on other types of surfaces and also application of optimization techniques to obtain the deposited layer of required geometry. Of great importance will also be modeling of residual mechanical strains and stresses for predicting the properties of the deposited layer and its life expectancy.

### Acknowledgment

This research has been supported by the Ministry of Education, Youth and Sports of the Czech Republic under the RICE New Technologies and Concepts for Smart Industrial Systems, project LO1607 and Faculty internal project No. SGS-2015-035.

**Authors:** Prof. Ing. Ivo Doležel, CSc., Assoc. Prof. Ing. Václav Kotlan, Ph.D., Ing. Roman Hamar, Ph.D., Ing. David Pánek, Ph.D., University of West Bohemia, Faculty of Electrical Engineering, Univerzitní 26, 306 14 Plzeň, Czech Republic, {idolezel, vkotlan, hamar, panek50}@kte.zcu.cz.

### REFERENCES

- [1] J. T. Hofman, D. F. de Lange, B. Pathiraj, J. Meier: FEM modeling and experimental verification for dilution control in laser cladding. *J. Material Processing Technology* 211 (2011), No. 2, 187–196.
- [2] F. Brückner, S. Nowotny, Ch. Leyens: Innovations in laser cladding and direct metal disposition. *Proc. SPIE 8239, High Power Laser Materials Processing: Lasers, Beam Delivery, Diagnostics, and Applications*, January 21, 2012, California, USA
- [3] H. Qi, J. Mazumder: Numerical simulation of heat transfer and fluid flow in coaxial laser cladding process for direct metal deposition. *Journal of Applied Physics*, 100 (2006), No. 2, paper 024903
- [4] Y. Fu, A. Loredó, B. Martin, A.B. Vannes: A theoretical model for laser and powder particles interaction during laser cladding. *J. Material Processing Technology* 128 (2002), Nos. 1–3, 106–112
- [5] M. Kuczmann, A. Iványi: The finite element method in magnetics. *Akadémiai Kiadó, Budapest* (2008)
- [6] J. A. Stratton: Electromagnetic theory. *Wiley-IEEE Press, New York* (2007)
- [7] J. P. Holman: Heat transfer, *McGraw-Hill, New York* (2002)
- [8] M. Courtois, M. Carin, P.L. Mason, S. Gaied, M. Balabane: A complete model of keyhole and melt pool dynamics to analyze instabilities and collapse during laser welding. *J. Laser Applications* 26 (2014), No. 4, paper 042001
- [9] B.R. Brandstatter, W. Ring, C. Magele, K.R. Richter: Shape design with great geometrical deformations using continuously moving finite element nodes. *IEEE Trans. Magn.* 34 (1998), No. 5, 2877–2880
- [10] Y. Zhao, S.L. Ho and W.N. Fu: A novel fast remesh-free mesh deformation method and its application on to optimal design of electromagnetic devices. *IEEE Trans. Magn.* 50 (2014), No. 1, 1–4